

# BARYON NUMBER TRANSFER IN NUCLEAR COLLISIONS AT SPS ENERGIES\*

ANDRZEJ RYBICKI

Henryk Niewodniczański Institute of Nuclear Physics  
Radzikowskiego 152, 31-342 Kraków, Poland

for the NA49 Collaboration

*(Received April 29, 2002)*

New data on identified baryons in the projectile hemisphere of  $p+p$  and centrality-selected  $p+Pb$  and  $Pb+Pb$  collisions are shown. Information from pion-induced interactions is used to isolate the projectile role in the observed phenomena. A common picture emerges for  $p+p$ ,  $p+Pb$  and  $Pb+Pb$  reactions: with increasing centrality, the projectile baryon number is strongly “pushed” towards the backward hemisphere of the collision. In the magnitude of this common effect, most central  $Pb+Pb$  interactions occupy a medium position between  $p+p$  and central  $p+Pb$  reactions.

PACS numbers: 25.75.-q, 12.38.Mh

## 1. Introduction

The NA49 experiment [1, 2] provides the possibility of exploring a wide range of hadronic interactions, starting with elementary hadron+proton processes via hadron+nucleus collisions with controlled centrality, up to nucleus+nucleus reactions. The large acceptance of the detector, particle identification over most of this acceptance, and large statistics of the collected data, allow for detailed comparative studies. Such a study is presented below for the process of baryon number transfer (baryon stopping) in  $p+p$ ,  $p+Pb$ , and  $Pb+Pb$  collisions. The analysis is performed at a single beam energy of 158 GeV/nucleon; it is based on longitudinal net proton ( $p - \bar{p}$ ) and net neutron ( $n - \bar{n}$ ) spectra. First, a comparison of elementary  $p+p$  and  $\pi+p$  interactions is made in order to identify the role of the projectile in

---

\* Presented at the Cracow Epiphany Conference on Quarks and Gluons in Extreme Conditions, Cracow, Poland, January 3-6, 2002.

the observed processes. This serves as a basis for a study of baryon stopping in  $p + \text{Pb}$  reactions, which are then compared to  $\text{Pb} + \text{Pb}$  collisions. The basic characteristics of baryon number transfer in the three reaction types are discussed.

## 2. Experimental procedure and data presentation

A detailed description of data analysis of hadron- and  $\text{Pb}$ -induced reactions can be found in [2] and [3], respectively. Below the most important aspects are discussed.

The identification of protons and antiprotons in the NA49 TPC system is achieved by measuring their specific energy loss in the TPC gas (the  $dE/dx$  method). The TPC acceptance extends over the proton  $x_F$  range of  $-0.1$  to  $0.5$ ; it covers the complete  $p_T$  range<sup>1</sup>. Neutrons are identified in a forward hadronic calorimeter covering the  $x_F$  range of  $0.2$  to  $1$ . As this device provides no possibility of distinguishing between neutrons and anti-neutrons, the assumption  $\bar{n} = \bar{p}$  has been applied to obtain  $n - \bar{n}$  spectra.

The centrality control in hadron+nucleus reactions is realised by measurement and triggering on the number of intermediate energy target protons (lab momentum range of  $0.15$  to  $1$   $\text{GeV}/c$ ). These “grey” protons are measured in a dedicated Centrality Detector [1], and additionally in the TPC system by the  $dE/dx$  method. The connection between the number of observed grey protons  $n_{\text{grey}}$  and the number of elementary subcollisions suffered by the projectile  $\nu$  is traced using the VENUS 4.12 event generator. Thus, each data sample selected by a given cut on  $n_{\text{grey}}$  is characterised by the corresponding mean number of elementary subcollisions,  $\langle \nu \rangle$ . In  $A + A$  collisions, the on-line centrality selection relies on the energy deposit of beam fragments in a forward zero degree calorimeter. The connection between this energy deposit and the number  $\nu$  of elementary subcollisions suffered by each nucleon participating in the  $A + A$  interaction, is again traced using VENUS. The number of participant nucleons is obtained by estimating the net baryon number carried by outgoing particles [4].

All the presented results are preliminary. The error bars shown are only statistical. Unless explicitly specified, all lines and curves drawn in the figures serve merely to guide the eye.

## 3. Elementary collisions

A good starting point for studying the phenomenon of baryon number transfer in hadronic collisions is the net proton  $x_F$  spectrum in inelastic  $p + p$  reactions. This spectrum is shown in Fig. 1; it will serve as a basis for the simple conjecture formulated below.

---

<sup>1</sup> Unless explicitly specified, all kinematical variables refer to the nucleon+nucleon c.m.s.

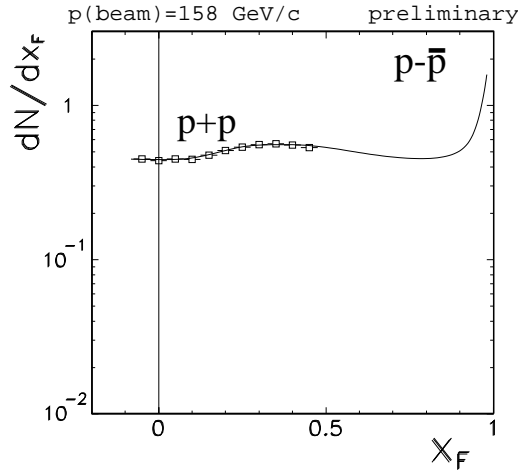


Fig. 1. Longitudinal net proton spectrum in inclusive (minimum bias) inelastic  $p+p$  collisions. Outside the limit of the TPC acceptance, the NA49 data (squares) are supplemented with a compilation of existing results (curve based on [5]).

Let us assume that we have full knowledge of the net baryon ( $B - \bar{B}$ ) distribution in  $p + p$  and  $\pi + p$  interactions. Let us conjecture that the  $\pi + p$  distribution behaves as shown in Fig. 2(a): it approaches the  $p + p$  spectrum in the backward region, reaches 1/2 of the  $p + p$  value at  $x_F = 0$ , and decreases in the forward direction. In such a case we would have reasons to suppose that the  $p + p$  spectrum can in fact be *separated*

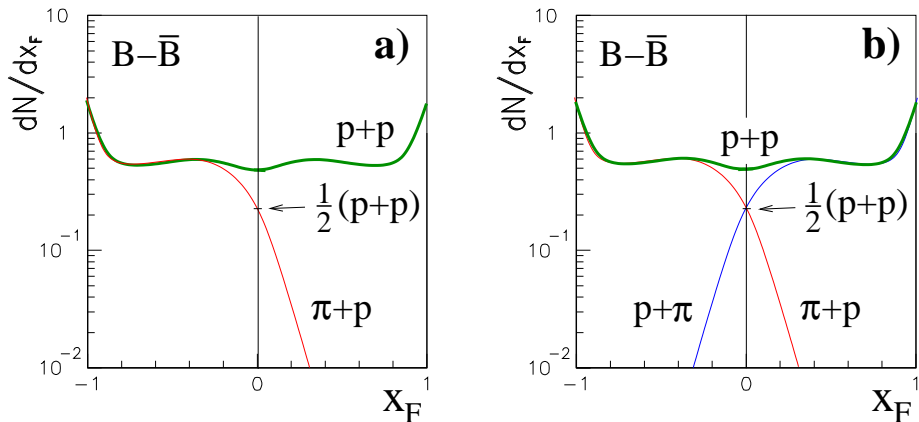


Fig. 2. (a) Hypothetical comparison of net baryon spectra in  $p + p$  and  $\pi + p$  reactions. (b) The same comparison, with a reflected ( $p + \pi$ ) curve added to the plot.

into two components, as shown in Fig. 2(b): the  $\pi + p$  distribution, and the reflected  $p + \pi$  spectrum. Since in  $p + p$  ( $p + \pi$ ) interactions the incoming net baryon number is carried uniquely by the proton target (projectile), we could draw the following conclusions:

- the net baryon spectrum in  $p + p$  reactions is a sum of two components which can be attributed to the target and to the projectile.
- the target component is identical in  $p + p$  and  $\pi + p$  reactions.
- it is possible to obtain the “pure” projectile component in  $p + p$  by subtracting the target component from the total spectrum.

The “two-component picture” formulated above is verified in Fig. 3 using experimental net proton spectra. The “ $\pi + p$ ” distribution shown in the figure is the mean value of net proton distributions in inclusive inelastic  $\pi^+ + p$  and  $\pi^- + p$  collisions<sup>2</sup>. At  $x_F = 0$ , the  $\pi + p$  spectrum reaches 1/2 of

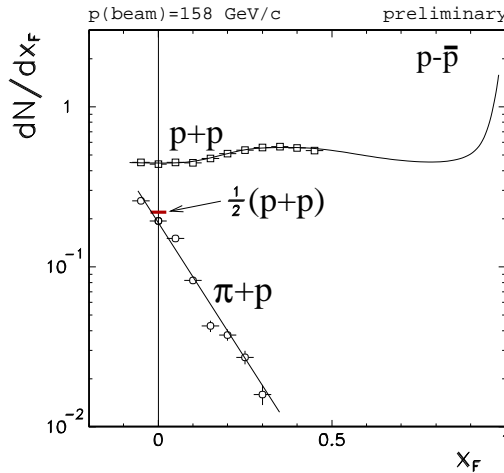


Fig. 3. Net proton spectrum in  $p + p$  reactions (shown before) and in  $\pi + p$  collisions (described in the text). At  $x_F = 0$ , 1/2 of the  $p + p$  value is marked.

the  $p + p$  value, within an accuracy comparable to the present estimate of experimental systematic errors. Within this accuracy, Fig. 3 repeats what has been shown in Fig. 2(a). Therefore, we can assume that the  $\pi + p$  net proton distribution indeed reflects the contribution of the target to the total  $p + p$  spectrum, and can be used to extract the projectile component of net proton spectra in  $p + p$  interactions. The same hypothesis will now be applied to explore the fate of the projectile baryon number in nuclear collisions.

<sup>2</sup> This average distribution is used to eliminate the effect of projectile isospin dependent baryon-antibaryon pair production discussed in [6].

#### 4. Baryon stopping in $p + A$ collisions

An extension of the two-component picture formulated in Section 3 is proposed in Fig. 4. Panel (a) shows the hypothetical behaviour of projectile and target components of the net baryon spectrum in a centrality-selected  $p + A$  reaction. The behaviour of the projectile component (P) is *a priori* unknown, but *baryon stopping* is expected: after the projectile has undergone multiple subcollisions with target nucleons, its contribution to the net baryon spectrum will change shape and become more central. For the target component (T), the simplest expectation possible is that it will pile up proportionally to the number of target nucleons hit by the projectile (*i.e.*, the number of elementary subcollisions  $\nu$ ). It should be noted that the projectile component can be accessed experimentally using  $\pi + A$  data (Fig. 4(b)) to subtract the contribution of the target.

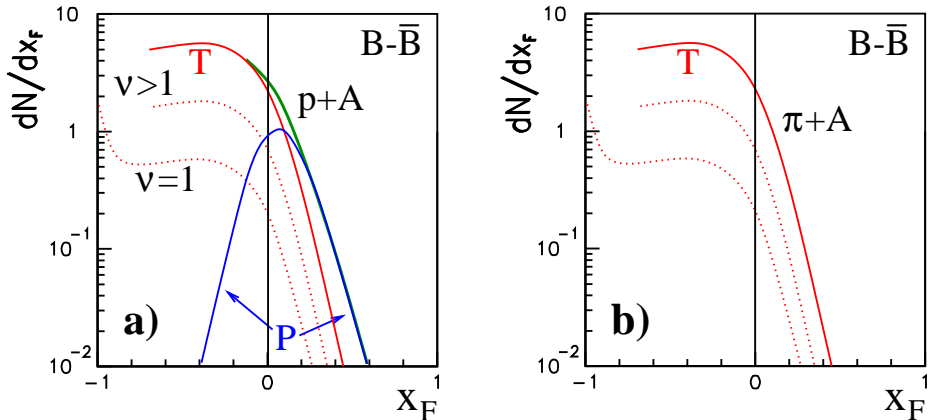


Fig. 4. (a) Hypothetical two-component picture of net baryon ( $B - \bar{B}$ ) spectrum in a  $p + A$  reaction at a given centrality. The total  $p + A$  spectrum is a sum of two components: T-target, P-projectile. The T component piles up proportionally to  $\nu$ , as shown in the plot. (b) The same for a  $\pi + A$  interaction. The total  $\pi + A$  net baryon spectrum contains only the target component.

It is interesting to verify whether the target component follows the simple expectation formulated above. This can be done by a direct study of  $\pi + \text{Pb}$  collisions, as shown in Fig. 5. Similarly to the  $\pi + p$  net proton spectrum from Section 3, the two “ $\pi + \text{Pb}$ ” distributions shown in the figure are averages of corresponding  $\pi^+ + \text{Pb}$  and  $\pi^- + \text{Pb}$  spectra. The general behaviour of the distributions is not far from the expected linear pile-up with  $\langle \nu \rangle$ , although a certain steepening of the  $p - \bar{p}$  spectrum is indicated by the data on most central  $\pi + \text{Pb}$  reactions.

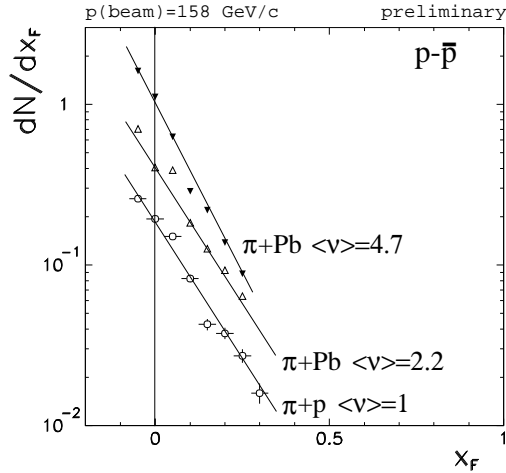


Fig. 5. Longitudinal net proton spectra in  $\pi + p$  reactions (shown before) and for two centrality-selected  $\pi + \text{Pb}$  samples (see description in the text). The two  $\pi + \text{Pb}$  samples are characterised by  $\langle \nu \rangle$  values obtained from the VENUS event generator (by definition,  $\langle \nu \rangle = 1$  in  $\pi + p$  collisions). The statistical error bars of the  $\pi + \text{Pb}$  distributions are not shown.

The experimental net proton spectra in  $p + p$  and centrality-selected  $p + \text{Pb}$  reactions are shown in Fig. 6. As expected from Fig. 4(a), a strong steepening of the total  $p - \bar{p}$  spectrum with increasing centrality is apparent. This results from two effects: the target component pile-up discussed above, and the change of projectile components' shape with increasing centrality.

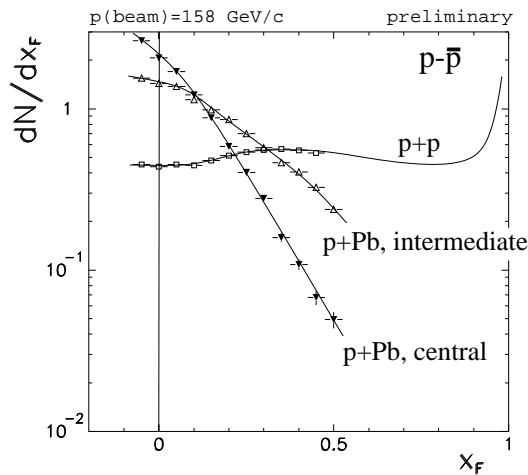


Fig. 6. Longitudinal net proton spectra in  $p + p$  collisions (shown before), for an intermediate centrality sample of  $p + \text{Pb}$  reactions, and for a central  $p + \text{Pb}$  sample.

In order to isolate the latter effect, the projectile components of the above spectra have been extracted, and are shown in Fig. 7. For  $p+p$  interactions, this has been done by subtracting the target component (the  $\pi+p$  distribution) from the total spectrum. For the two  $p+Pb$  centrality samples, net proton distributions from the corresponding  $\pi+Pb$  centrality samples have been subtracted (see [2] for more details).

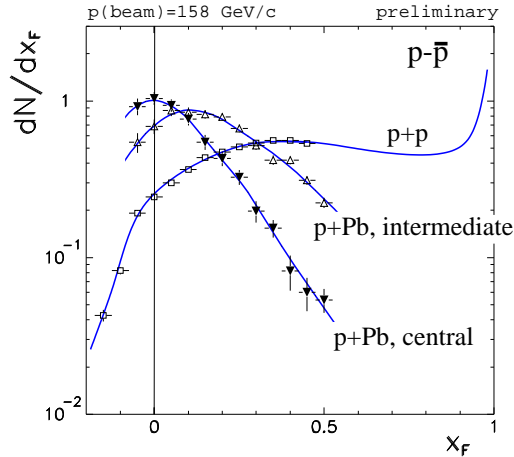


Fig. 7. Projectile components of net proton spectra in  $p+p$ , intermediate  $p+Pb$ , and central  $p+Pb$  reactions.

As can be seen from Fig. 7, a strong “push” of projectile baryon number towards the backward hemisphere is observed with increasing centrality of the  $p+Pb$  reaction. In  $p+p$  interactions, the projectile component of the  $p-\bar{p}$  spectrum is mostly “flattish” and well localised in the forward hemisphere of the collision; in central  $p+Pb$  reactions, the bulk of it appears concentrated in the vicinity of  $x_F = 0$ . Between  $p+p$  and central  $p+Pb$  collisions, the projectile baryon number density at  $x_F = 0$  increases by a factor of four. Thus, the observed baryon stopping effect will strongly influence the mid-rapidity  $\bar{p}/p$  ratio.

It should be underlined that the whole discussion of baryon stopping made up to now has been based on net *proton* spectra. This implies the assumption that these spectra are representative of total net *baryon* distributions — that there is no basic difference between, *e.g.*, final state protons and neutrons. The NA49 experiment has the possibility to check the validity of this assumption by a study of net neutron spectra shown in Fig. 8. As it appears, the observed “push” of projectile baryon number is not specific to final state protons: a very similar effect is observed for final state neutrons<sup>3</sup>.

<sup>3</sup> Note: the target component has *not* been subtracted from net neutron spectra shown in Fig. 8. However, its contribution will be small above  $x_F = 0.3$ .

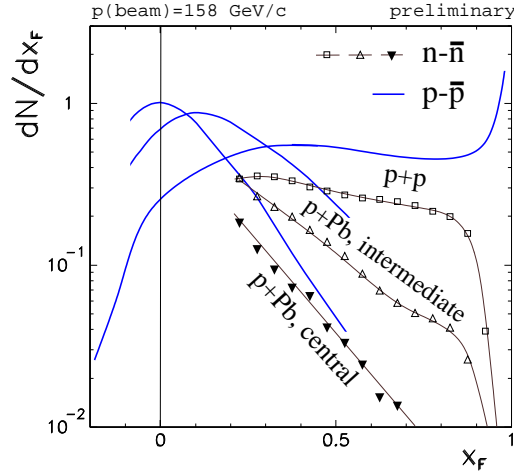


Fig. 8. Data points:  $n - \bar{n}$  spectra in  $p + p$ , intermediate  $p + \text{Pb}$ , and central  $p + \text{Pb}$  collisions. Curves: projectile components of  $p - \bar{p}$  spectra in  $p + p$ , intermediate  $p + \text{Pb}$ , and central  $p + \text{Pb}$  reactions (shown in Fig. 7).

### 5. Comparison to $A + A$ reactions

The analysis made in the previous section brings an important benefit in comparisons between  $p + A$  and  $A + A$  interactions. In an  $A + A$  reaction, both projectile and target nucleons suffer multiple subcollisions. In a  $p + A$  reaction, only the projectile suffers multiple subcollisions; its contribution to the observed effects is “hidden” in the total spectra, strongly influenced by target nucleons. The study made in Section 4 provides a way to solve this problem: once projectile components of net proton spectra in  $p + A$  and  $A + A$  collisions are extracted, they can be compared directly.

Fig. 9 shows participant-scaled net proton distributions in centrality-selected  $\text{Pb} + \text{Pb}$  collisions,  $\langle \nu \rangle \approx 4.6$  being the highest centrality sample practically accessible in  $\text{Pb} + \text{Pb}$  reactions. The reference “ $N + N$ ” curve shown in the figure is the corresponding  $p - \bar{p}$  distribution in elementary nucleon+nucleon collisions, which takes account of the isospin content of the  $\text{Pb}$  nucleus (39% protons and 61% neutrons). It is constructed as a weighted sum of net proton and net neutron spectra measured in  $p + p$  reactions:

$$N + N \rightarrow (p - \bar{p})X = 0.39 \left( p + p \rightarrow (p - \bar{p})X \right) + 0.61 \left( p + p \rightarrow (n - \bar{n})X \right).$$

In order to extend the analysis made in the preceding section to  $\text{Pb} + \text{Pb}$  interactions, the projectile component of  $p - \bar{p}$  spectra shown in Fig. 9 has to be extracted. It should be underlined that the target subtraction procedure based on pion-induced reactions, used for  $p + p$  and  $p + A$  collisions cannot

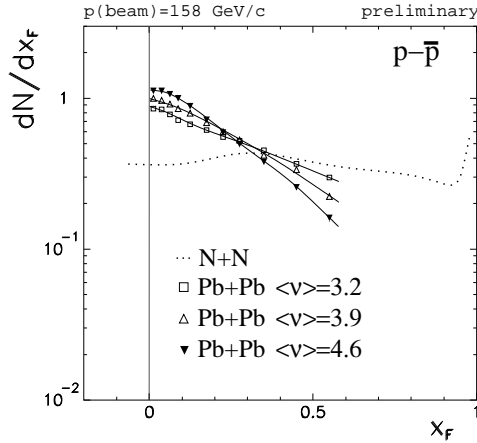


Fig. 9. Net proton spectra in three centrality-selected Pb + Pb samples, together with the elementary reference  $N + N$  curve described in the text. Each of the Pb + Pb distributions is scaled down by the corresponding number of participant pairs, and characterised by a  $\langle \nu \rangle$  value obtained from VENUS.

be directly extended to  $A + A$  interactions<sup>4</sup>. However, as illustrated in Fig. 10, a symmetry constraint can be imposed on the projectile and target components of the total  $p - \bar{p}$  spectrum in  $A + A$  collisions: they must be

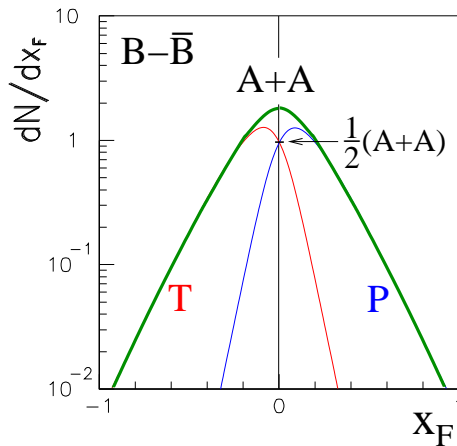


Fig. 10. Hypothetical two-component picture of net baryon spectrum in  $A + A$  reactions. The total  $A + A$  spectrum is a sum of two symmetric components (T-target, P-projectile). Note: at  $x_f = 0$ , the value of both components must be equal to  $1/2$  of the total  $A + A$  value.

<sup>4</sup> The logical extension of this procedure to  $A + A$  data would imply the use of a nuclear projectile containing no baryon number, a “pion nucleus” which does not exist.

equal at  $x_F = 0$ . With this constraint, their shape can be deduced on the basis of  $\pi + p$  and  $\pi + \text{Pb}$  interactions: as a first approximation, appropriately scaled net proton distributions from  $\pi + \text{Pb}$  reactions can be used to subtract the target component (see [2] for more details). This gives the projectile components of net proton spectra in  $\text{Pb} + \text{Pb}$  collisions, shown in Fig. 11. The projectile component of the  $N + N$  reference curve is deduced on the basis of  $p - \bar{p}$  spectra in  $p + p$  interactions.

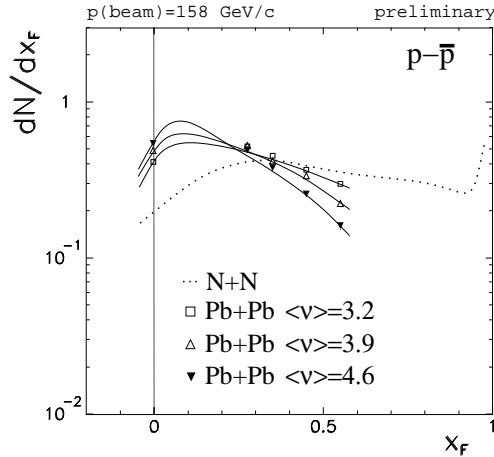


Fig. 11. Projectile components of net proton spectra in centrality-selected  $\text{Pb} + \text{Pb}$  reactions, and projectile component of the elementary  $N + N$  curve.

The overall picture of baryon stopping in  $\text{Pb} + \text{Pb}$  collisions, presented in Fig. 11, can be compared to that shown for  $p + \text{Pb}$  reactions (Fig. 7). The two pictures are similar. With increasing centrality, the “flattish” elementary spectrum steepens and is “pushed” towards  $x_F = 0$ . A direct comparison of the two sets of distributions is not straightforward, due to differences between the reference  $p + p$  and  $N + N$  curves. An attempt at such a comparison is proposed in Fig. 12, where the  $N + N$  curve is scaled up by an arbitrary factor to match the  $p + p$  curve “as well as possible”. The same scaling factor is applied to the  $\text{Pb} + \text{Pb}$  distributions.

The comparison made in Fig. 12 gives a clear result. In  $p + \text{Pb}$  and  $\text{Pb} + \text{Pb}$  reactions, the evolution of projectile components with centrality is so similar that the two sets of curves form a *single, smooth pattern*. Thus, a *common picture of baryon stopping in  $p + p$ ,  $p + \text{Pb}$  and  $\text{Pb} + \text{Pb}$  collisions* emerges from the figure: with increasing centrality, the projectile baryon number is smoothly “pushed” towards the backward hemisphere. In this common picture, central  $\text{Pb} + \text{Pb}$  collisions occupy a *medium position* between  $p + p$  and central  $p + \text{Pb}$  reactions; this is not surprising and can be understood from simple geometrical considerations. If we assume that a  $\text{Pb} + \text{Pb}$  reaction

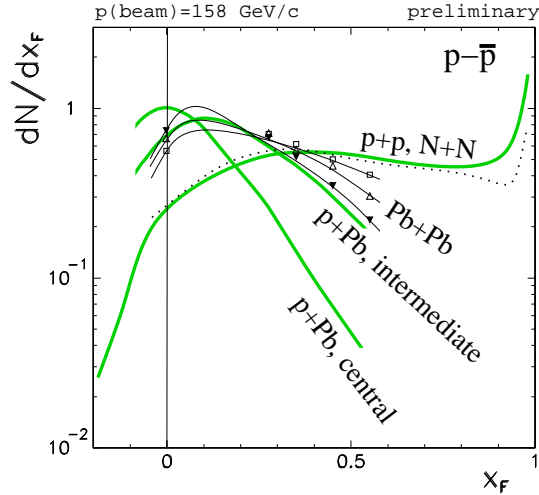


Fig. 12. Comparison of projectile components of net proton spectra in  $p + \text{Pb}$  and  $\text{Pb} + \text{Pb}$  reactions. The  $p + p$  and  $p + \text{Pb}$  results from Fig. 7 are represented by shaded curves. The  $N + N$  and  $\text{Pb} + \text{Pb}$  spectra from Fig. 11 (dotted and solid curves) are scaled up by a common factor as described in the text.

is a superposition of nucleon+ $\text{Pb}$  collisions, a central  $\text{Pb} + \text{Pb}$  interaction will be composed of both central and peripheral collisions. As a direct consequence, less stopping than in a central  $p + \text{Pb}$  collision is expected.

### 6. Summary

A comparative study of net proton and net neutron spectra in elementary and nuclear collisions has been presented, offering insight into baryon stopping processes in  $p + p$ ,  $p + \text{Pb}$ , and  $\text{Pb} + \text{Pb}$  interactions. The two-component hypothesis appears consistent with the data on elementary reactions: the net proton spectrum in  $p + p$  collisions can be described as sum of projectile and target components, which can be separated using data on  $\pi + p$  reactions.

The same two-component hypothesis has been applied to centrality-selected nuclear collisions. This has resulted in a common picture of baryon stopping in  $p + p$ ,  $p + \text{Pb}$ , and  $\text{Pb} + \text{Pb}$  reactions. With increasing centrality, the projectile baryon number is smoothly “pushed” towards the backward hemisphere of the collision; this phenomenon is very similar for  $p + \text{Pb}$  and  $\text{Pb} + \text{Pb}$  interactions. In the magnitude of this common effect, most central  $\text{Pb} + \text{Pb}$  collisions occupy a medium position between  $p + p$  and central  $p + \text{Pb}$  reactions.

This work was supported by the Polish State Committee for Scientific Research (KBN) under grant no. 2 P03B 02418.

## REFERENCES

- [1] S. Afanasev *et al.*, NA49 Collaboration, *Nucl. Instrum. Methods Phys. Res.* **A430**, 210 (1999).
- [2] A. Rybicki, Ph.D. Thesis, <http://na49info.cern.ch>.
- [3] J. Bächler *et al.*, NA49 Collaboration, *Nucl. Phys.* **A661**, 45c (1999).
- [4] G.E. Cooper, NA49 Collaboration, *Nucl. Phys.* **A661**, 362c (1999).
- [5] J. Whitmore, S.J. Barish, D.C. Colley, P.F. Schultz, *Phys. Rev.* **D11**, 3124 (1975); J. Whitmore, *Phys. Rep.* **10**, 273 (1974); M.G. Albrow *et al.*, CHLM Collaboration, *Nucl. Phys.* **B108**, 1 (1976); M.G. Albrow *et al.*, CHLM Collaboration, *Nucl. Phys.* **B73**, 40 (1974).
- [6] H.G. Fischer, NA49 Collaboration, *Acta Phys. Pol.* **B33**, 1473 (2002).